

Magnetoresistance of Junctions made of Underdoped YBCO Separated by a Ga-doped YBCO Barrier

L. Shkedy, G. Koren and E. Polturak

Physics Department, Technion – Israel Institute of Technology Haifa, 32000, ISRAEL

(Dated: March 22, 2024)

We report magnetoresistance measurements of ramp type superconductor-normal-superconductor (SNS) junctions. The junctions consist of underdoped $\text{YBa}_2\text{Cu}_3\text{O}_y$ (YBCO) electrodes separated by a barrier of $\text{YBa}_2\text{Cu}_{2.6}\text{Ga}_{0.4}\text{O}_y$. We observe a large positive magnetoresistance, linear in the field. We suggest that this unusual magnetoresistance originates in the field dependence of the proximity effect. Our results indicate that in underdoped YBCO/N/YBCO SNS structures, the proximity effect does not exhibit the anomalously long range found in optimally doped YBCO structures. From our data we obtain the diffusion coefficient and relaxation time of quasiparticles in underdoped YBCO.

PACS numbers: 74.45.+c, 74.25.Ha

INTRODUCTION

In the usual description of the proximity effect, when a superconductor (S) is brought into contact with a normal conductor (N), the order parameter (OP) in the superconductor is depressed near the interface and superconductivity is induced in N. The pair amplitude induced in N decays on a length scale K^{-1} from the interface, called the decay length [1, 2, 3]. In SNS junctions in which S is an optimally doped HTSC and N belongs to the same material family, but is doped to be non superconducting, the decay of the pair amplitude in N typically takes place over a rather long distance of tens of nm, [4, 5]. In contrast, if both S and N are underdoped cuprates, the pair amplitude in N seems to decay over a much shorter distance, on the order of a few nm. We have observed this effect in underdoped YBCO based junctions [6, 7] having a barrier made of $\text{YBa}_2\text{Cu}_{2.55}\text{Fe}_{0.5}\text{O}_y$ or a $\text{YBa}_2\text{Cu}_{2.6}\text{Ga}_{0.4}\text{O}_y$. In SNS junctions having a barrier much thicker than the decay length, Cooper pairs cannot tunnel through and the junctions exhibit a finite resistance at all temperatures. Roughly speaking, superconductivity in N is induced near the two SN interfaces, while a section of length ℓ in the middle of the barrier remains normal. This is the type of junction studied in the present work.

We are not aware of previous investigations of the proximity effect in HTSC under a magnetic field. When a magnetic field is applied, superconductivity is reduced and penetrates less into the normal conductor. As a result, the proximity effect is field dependent [2]. If the superconductivity in the barrier is weakened, the length of the normal section in the junction should increase, and with it the junction's finite resistance. As a result, a positive magnetoresistance (MR, defined as $\text{MR} = (R(H) - R(0))/R(0)$) should be observed. We indeed observed such MR, linear in the field. An attempt to explain this unusual field dependence is the subject of this

paper.

Besides the field dependence of the proximity effect, there are several additional mechanisms which could contribute to the MR. These include flux flow in the superconducting electrodes [3, 10], normal MR of the barrier material which is caused by bending of electron trajectories [11], field dependent hopping in the barrier [12, 13], and resonant tunneling between the electrodes across the barrier [14]. In the following we show that the contribution of all these processes to the observed MR is insignificant and we attribute it primarily to a field dependent proximity effect in the barrier.

EXPERIMENTAL

The junctions used in the present study are thin In based ramp junctions of the type that was previously used in our work [6]. The junctions consist of two underdoped superconducting YBCO electrodes separated by a thin layer of Ga-doped YBCO barrier. Ga has no magnetic properties. The transport current flows in the a-b plane through the Ga-doped YBCO layer. The multi-step process of junction preparation by laser ablation was described previously [6]. Briefly, we first deposit a 100 nm thick c-axis oriented epitaxial YBCO layer onto a (100) SrTiO_3 (STO) substrate. This base electrode is then capped by a thick insulating layer of STO. Patterning is done by Ar ion milling to create shallow angle ramps along a main crystallographic direction in the a-b plane. In a second deposition step, the barrier layer, the YBCO cover electrode and the Au electrical contacts are deposited, and then patterned to form the final junctions layout. This produces several junctions with 5 mm width on the wafer. Four terminal resistance measurements of the junctions were carried out as a function of temperature and magnetic field of up to 8 Tesla. The field was perpendicular to the transport current, which in our geometry flows in the a-b plane of the In s.

Electronic address: lior_shk@physics.technion.ac.il

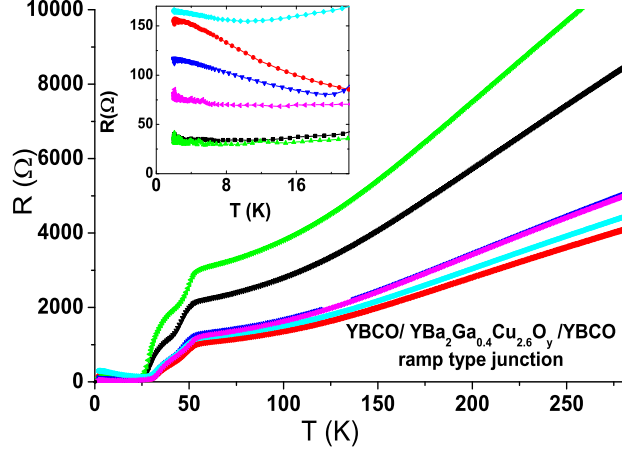


FIG. 1: (Color online) Resistance versus temperature of six junctions with 21nm thick Ga-doped YBCO barrier. In the normal state, the different resistances of the junctions are due to different lengths of the YBCO leads. The inset shows the low temperature resistance of the junctions where both electrodes are superconducting.

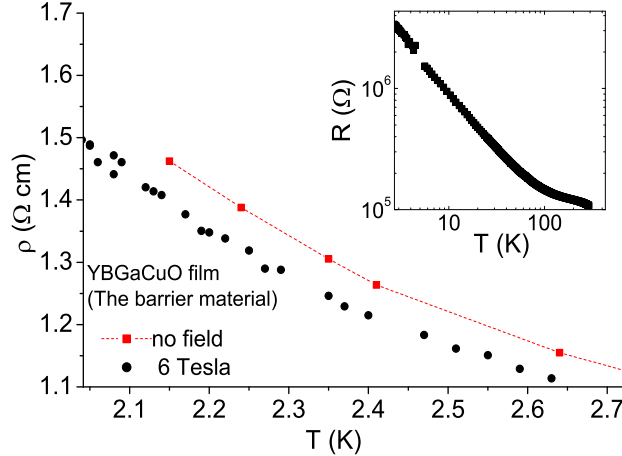


FIG. 2: (Color online) Resistivity versus temperature of 100nm thick film of the Ga-doped YBCO material. Square symbols are measured at zero field and the circles are measured with 6 Tesla field applied perpendicular to the film. Note that the MR of the film is negative, in contrast to the positive MR of our junctions.

RESULTS AND DISCUSSION

Resistance versus temperature (RT) measurements of six junctions on the wafer are shown in Fig. 1. In the normal region, the difference in the resistance of the junctions is due to the different lengths of the YBCO leads. One observes two distinct superconducting transitions with T_c onset of 35K and 53K which are

attributed to each one of the electrodes. In the oxygen annealing process of underdoped YBCO, the oxygen concentration is kept low and the duration of the annealing is relatively short. Consequently, the base electrode which is covered by a thick layer of STO, absorbs less oxygen and its transition temperature is lower. Below about 30K, both electrodes are superconducting and the inset of Fig.1 shows the low temperature resistance of the junctions, which is due to the barrier. Qualitatively similar behaviour was observed in edge junctions made of underdoped YBCO separated by a $\text{YBa}_2\text{Cu}_{2.55}\text{Fe}_{0.5}\text{O}_y$ barrier [6, 7]. The scatter of the values between different junctions is typical of our junction preparation process, and is probably due to nonuniformities in the local Ga concentration, and to variations in the transparency of the interfaces, most probably resulting from damage created by the ion milling of the ramp. The transparency of our junctions can be estimated from measurements of the critical current described below, which indicate that the transparency is low. The temperature dependence of the junction's resistance is typically weaker than that of the parent material in the form of a film, shown in Fig. 2. At low temperatures, the absolute resistivity of the junctions is also much smaller than that of a $\text{YBa}_2\text{Cu}_{2.6}\text{Ga}_{0.4}\text{O}_y$ film. One possible interpretation is that the thickness of the barrier (21 nm in this work) is in the range where the material is mesoscopic. Under these conditions, the temperature dependence of the resistance is expected to be much weaker than that of a macroscopic film [15]. The differences of the absolute resistivities between different junctions may perhaps result from different interface transparency, which also affect the conductance of the device in the mesoscopic regime [15].

Our main experimental result is shown in Fig. 3, where the measured magnetoresistance MR at low T is plotted as a function of magnetic field normal to the wafer. All junctions showed similar behavior. Detailed measurements were done on three of the six junctions on the wafer. One can see that all three junctions show a large positive MR which is linear in the applied field. The MR typically reaches a value of 20 at 8 Tesla, which is larger than the resistance at $H=0$ by tens of percent.

We consider possible sources for the MR in our junctions. MR originating in the two YBCO electrodes below the superconducting transition temperature can result for instance from flux motion. This contribution would be linear in the field. In order to estimate the size of this contribution, we performed low temperature MR measurements on bare YBCO microbridges. At temperatures close to T_c , flux flow was indeed observed (see Appendix). However, at low temperatures where the junctions of Fig. 3 were measured, no measurable MR was observed in the thin film YBCO microbridges. Therefore, flux flow in the YBCO electrodes does not

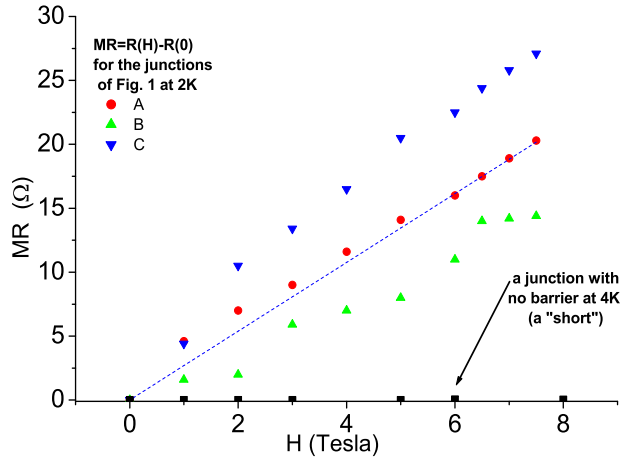


FIG. 3: (Color online) Magnetoresistance versus field of three of the junctions of Fig. 1 at 2K, and of a "short" junction at 4K. The "short" resistance is of about 0.4 Ω at 8 Tesla which is almost two orders of magnitude smaller than the corresponding MR of the other junctions with a barrier. The dashed line is a guide to the eye.

contribute to the MR. We also measured the MR of junctions prepared in the same way, but without the barrier layer. These junctions are referred to as "shorts". As shown in Fig. 3, under similar bias currents and fields, the "shorts" did exhibit a small MR of about 0.4 Ω at 8 Tesla. The "shorts" show a finite MR since the interface between the two YBCO electrodes is always in perfect. The MR of the "shorts" is smaller than the MR in the junctions by almost two orders of magnitude. The interface resistance cannot be directly measured. What can be measured is the critical current density. Typically, the critical current density at low temperature of a 60K YBCO "short" is one order of magnitude smaller than that of a μm . This implies that the transparency of our junctions is low. To summarize this section, the above series of control experiments show that MR in the electrodes is not the source of the large MR observed in our junctions.

A second potential source for the observed MR in Fig. 3 could be the barrier material itself. We therefore measured the MR of the Ga-doped YBCO. Specifically, we measured the resistance versus temperature of microbridges patterned in a thin μm of this material annealed under the same conditions as the junctions in Fig. 3. Fig. 2 shows the resistivity of these bridges with and without magnetic field. The barrier material exhibits a clear negative MR of 5% at 2K. The sign of this MR is opposite to that of the junctions which show a large positive MR. At low temperatures, where the MR of the Ga-doped μm s is largest, the MR contributed by the barrier in the junctions would be

at most -8% (5% of 160 Ω , as seen in the inset of Fig. 1). However, since the sign of the MR of the barrier material itself is negative, the net (positive) MR of the junctions should be even larger than shown in Fig. 3. Consequently, the properties of the barrier material on its own cannot explain the observed MR of the junctions.

The above mentioned control experiments clearly show that the MR of our junctions does not originate from the superconducting electrodes nor from the normal properties of the barrier material. The net MR which we see has a magnitude characteristic of the transition of part of the barrier from a superconducting to a normal state. We therefore examine whether the MR could originate from the depression of superconductivity near the SN interface of the junction.

Before going into a more detailed analysis, we note that our barrier is a mesoscopic section of a Mott insulator (MI), with the conductance of the material in bulk form showing variable range hopping [16]. Its low temperature resistivity, 0.8 Ωcm , is about 3 orders of magnitude larger than the maximum resistivity of metals (Mott-Ioffe-Regel limit [22]). Strictly speaking, our junctions are S/M I/S junctions. So, the application of the usual theoretical description of the proximity effect to our junctions is not a priori justified, since both the de-Gennes and Usadel equations are valid only for dirty metals. However, it is an experimental fact that when an MI with resistivity $> 1\text{ cm}$ is in good electrical contact with a superconductor it behaves similarly to a metal [16, 23, 24, 25]. The question which particular model to use is therefore a matter of choice. In the limit of small induced pair amplitude in N, which applies to our low transparency junctions, the de-Gennes and Usadel approach give the same result. Since the de-Gennes approach was traditionally employed in all previous and current work on HTSC proximity structures [4, 9, 26], we prefer to follow this route. In any case, the analysis presented below is nevertheless useful, in terms of assigning values to physical quantities such as the decay length which can then be inter-compared between different experiments.

We first discuss the MR on the S side of the SN interface. In this region, the order parameter is reduced, superconductivity is depressed, pinning is weakened and flux flow could occur despite the low temperature. We now estimate the upper limit on the contribution of this effect to the MR. The low temperature normal state resistivity of YBCO, extrapolated from the linear part of the RT plot above the transition, is about 10^{-4} cm . An upper limit on the volume near the interface in which superconductivity is weakened is $10^{-4}\text{ A} \times 200\text{ A} \times 0.5\text{ m}^2$, where A is the junction cross section [21]. The normal state resistance of this region is very low, less than 0.1 Ω . Since the flux flow resistance is a fraction of the normal state resistance, it follows that

the MR in the S side close to the interface is negligible.

Turning now to the N side of the interface, the resistivity of the barrier material is quite high, $0.8 \text{ m}\Omega$ at 2K . A rough estimate done assuming Ohm's law in the barrier indicates that a 1 nm thick slice of the barrier has a resistance of $R = 16$. This value is similar to the total MR seen in Fig. 3. In the following, we propose that the observed MR is caused by changes in the effective penetration of superconductivity into the barrier. In other words, when a magnetic field is applied, the magnitude of the pair amplitude induced in the barrier is decreased and λ , the effective length of the barrier which remains normal, increases thus increasing the resistance of the junction.

The magnetic fields used in the present study are small compared with H_{c2} of the 60K YBCO phase which is 50T [20]. Thus changes in the minigap due to the applied field are also small but not negligible. The value of Δ on the S side near the interface is proportional to T_c which itself depends on the magnetic field due to pair breaking according to [3, 18].

$$\ln \frac{T_c}{T_{c0}} = \frac{1}{2} - \frac{1}{2} + \frac{1}{2 k_B T_c} \quad (1)$$

where T_c is the critical temperature under applied field and T_{c0} is the critical temperature at zero field. Δ is the digamma function defined as $\Delta(x) = \psi(x) = \Delta_0(x)$, and Δ_0 is the pair breaking parameter. For a thin film under perpendicular applied field $H = D_S eH = c$, where D_S is the diffusion coefficient in the superconductor. Since the highest magnetic field we used is small compared with H_{c2} , pair breaking is small and $\Delta_0 = 2 k_B T_c$ is a small parameter. In this limit, Eq. (1) reduces to [3, 18]

$$k_B (T_{c0} - T_c) = \frac{1}{4} \quad (2)$$

From our RT measurements under different fields we find the values of T_{c0} and T_c (65K at 0T and 55K at 7T , respectively). We can thus calculate the value of Δ_0 which is 1 meV at 7 Tesla . Therefore, $\Delta_0 = 2 k_B T_c = 1.35$, and this justifies the use of Eq. (2). By assuming a linear scaling between Δ_0 and T_c ($\Delta_0 = k_B T_c$, with k being a constant of about 5), we estimate that under a field of 7T the magnitude of Δ_0 decreases by about 15%. The suppression of Δ_0 can be therefore written as

$$\Delta_S = \Delta_S(0) - \Delta_S(H) = \frac{1}{8} = \frac{1}{8} \frac{D_S eH}{c} \quad (3)$$

where Δ_S is small compared with $\Delta_S(0)$. The spatial dependence of the Δ in an SNS junction is shown schematically in Fig. 4. The value of the Δ on both side of the interface are related through the standard boundary condition [2, 3]:

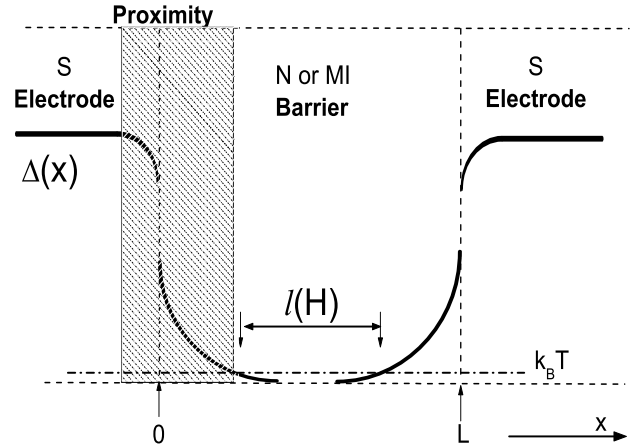


FIG. 4: A schematic diagram of the junction and the spatial profile of $\Delta(x)$. $\lambda(H)$ is the length of the resistive region of the junction. The shaded area shows the region in which superconductivity is weakened on both sides of the interface due to the proximity effect.

$$\frac{\Delta_S}{N_S V_S} \Big|_{x=0} = \frac{\Delta_N}{N_N V_N} \Big|_{x=0} \quad (4)$$

where Δ_S and Δ_N are the values of the minigap at the S and N sides of the SN interface. N_S and N_N are the normal state density of states (DOS) on the S and N sides of the interface, respectively. Finally, V_S and V_N are the electron-electron interaction on the S and N sides. Assuming the DOS and the electron-electron interaction are field independent we obtain

$$\frac{\Delta_S(H)}{\Delta_N(H)} = \frac{\Delta_S}{\Delta_N} \quad (5)$$

where $\Delta = N_S V_S = N_N V_N$ is a field independent constant and we define $\Delta_N(0) = \Delta_N(H)$. Δ_N which is the value at the interface, is also a small parameter as $\Delta_N = \Delta_N(0) < 1$.

Turning to the N side now, under a magnetic field H applied in the c -direction, the spatial dependence of Δ is given by the linearized Ginzburg-Landau (GL) equation [2]

$$\frac{d^2 \Delta_N}{dx^2} + \frac{2eH}{\hbar c}^2 (x_0 - x)^2 \Delta_N + K^2 \Delta_N = 0 \quad (6)$$

where x_0 and K are constants. In our experiment, $x_0 - x$ is limited by 10 nm which is half the thickness of our junction, the field H is less than 8T , and K is on the order of a few nm^{-1} . Using these parameters, we estimate that

the upper limit of the second term in Eq. (8) is about two orders of magnitude smaller than the last term. In this limit, the solution of Eq. (8) for i_N exhibits an exponential decay with distance $i_N(x) = \frac{i_N}{K} \exp(-Kx)$. In the dirty limit [2], K is given by

$$K^{-1} = \frac{\sim D_N}{2 k_B T} : \quad (7)$$

In this limit, where the cyclotron radius in the magnetic field is much larger than the mean free path, D_N is field independent and thus K does not depend on field. However, the value of i_N at the interface i_N , is field dependent because it is pinned to the value of the i_S on the S side at the interface i_S through Eq. (5). The pair amplitude induced in the barrier is effectively depressed to zero by thermal fluctuations at some distance from the interface, and from that distance onwards the material has a finite resistance. The natural way to determine this distance is through the condition that the extrapolated magnitude of i_N there is of the order of $k_B T$. This length, which we denote by X , depends on the field as

$$k_B T = \frac{i_N}{N} (H) e^{K X(H)} \quad (8)$$

where $X(H)$ is the effective penetration depth of superconductivity into N when a magnetic field is applied. Dividing the Eq. (9) for $X(H)$ by the equation for $X(H=0)$ we find

$$\frac{\frac{i_N}{N}(0)}{\frac{i_N}{N}(H)} = e^{K[X(H) - X(0)]} \quad (9)$$

and

$$X(H) - X(0) = \frac{1}{K} \ln \left(1 - \frac{\frac{i_N}{N}}{\frac{i_N}{N}(0)} \right) : \quad (10)$$

Since $\frac{i_N}{N}$ is a small parameter $X(H) - X(0) = \frac{1}{K} \ln \left(1 - \frac{\frac{i_N}{N}}{\frac{i_N}{N}(0)} \right)$. Referring to the schematic model shown in Fig. 4, the field dependent resistance of the barrier is $R = \lambda(H)/A$, where $\lambda(H) = L - 2X(H)$ is the length inside the barrier which is normal. Using Eq. (5) and the relation $2\lambda_S = k_B T_c$, the magnetoresistance comes out as

$$\begin{aligned} MR = R(H) - R(0) &= \frac{2}{A} (X(H) - X(0)) \quad (11) \\ &= \frac{e D_S}{2 c A K} \frac{1}{k_B T_c} H \end{aligned}$$

We therefore see that the MR is linear in H , in agreement with the observed behavior in Fig. 2.

A rough estimate of the decay length ($1=K$) in the underdoped barrier at low temperature can be

attempted using the resistivity of the barrier, 0.8 cm and the typical resistance of the junctions $100 \text{ } \Omega$. Using these values, we estimate the length of the barrier which remains normal ($H=0$) as 6 nm . Taking the thickness of the barrier of 21 nm , and assuming that the pair amplitude decays to zero over 3 times the decay length ($1=K$), we obtain a value for $1=K$ of about 2.5 nm . $1=K$ can also be calculated using Eq. (7), where $D_N = \frac{1}{3} \lambda_N v_{FN}$. The mean free path in the barrier can be estimated as the distance between nearest Ga atoms $\lambda_N = 5 \text{ \AA}$ and the Fermi velocity in the barrier $v_{FN} = 1.2 \cdot 10^7 \text{ cm/sec}$ was measured in a previous study [16]. This yields $1=K = 3.5 \text{ nm}$. It appears that both methods of estimating $1=K$ give values which are consistent. We note that the decay length estimated in underdoped SNS structure comes out much smaller than in optimally doped ones [4, 9].

Using our data we estimate the diffusion coefficient D_S and the relaxation time τ_S of underdoped YBCO. Taking an average T_c of 45 K , and an average slope in Fig. 3 of $MR/H = 2.7 \text{ mT}^{-1}$, Eq. (11) yields $D_S = 1 \text{ cm}^2/\text{sec}$. This is consistent with an independent estimate that can be extracted from Eq. (2) and from the relation between λ_S and the diffusion coefficient D_S which yields $1.7 \text{ cm}^2/\text{sec}$. The relaxation time, τ_S is extracted from the usual relation that connects it with the diffusion coefficient $D_S = \frac{1}{3} v_{FS}^2 \tau_S$ where v_{FS} is the Fermi velocity of quasiparticles in the superconductor $2 \cdot 10^7 \text{ cm/sec}$ [27]. Under these assumptions τ_S for YBCO is 25 fs . The value found for τ_S is of the same order of magnitude as the recent results of Gedik et al. who obtained $\tau_S = 100 \text{ fs}$ [27] while our value of D_S is smaller by than theirs, $D_S = 20 \text{ cm}^2/\text{s}$.

For completeness, we mention that Abrikosov has predicted another mechanism for linear MR versus H in superconductors [14]. He assumed a field dependent resonant tunneling which yields MR linear in H at very high magnetic fields, when only a few Landau levels are filled. When the field is reduced and the number of filled Landau levels increases the field dependence of the MR changes into a quadratic one. This model could in principle, explain the observed linear behavior of our MR results. However, peaks in the density of states due to Landau levels are absent in the dynamic resistance spectra of our junctions. Moreover, the fields used in our experiment are not high enough to reach the regime where a low number of Landau levels are filled. Hence, if this model was applicable to our junctions, we should have observed a quadratic dependence of the MR on field, which is not the case.

CONCLUSIONS

We investigated the resistance of SNS structures based on underdoped YBCO with non-magnetic Ga-doped YBCO barrier as a function magnetic field. We discovered a linear increase of the resistance with the field

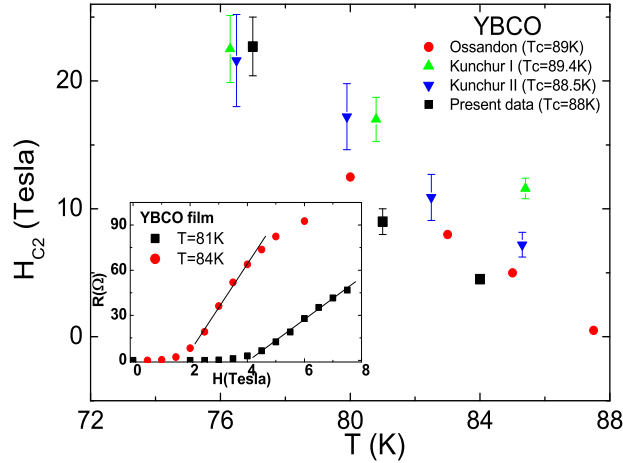


FIG. 5: (Color online) H_{c2} versus temperature of optimally doped YBCO film. H_{c2} was extracted from the slope of the linear part of the MR (inset) using the Bardeen-Stephen model. Our data (solid squares) can be compared with previous measurements by Kunchur et al. and Ossandon [29, 30].

MR. An extensive series of control experiments indicates that this field dependence does not result from flux flow, which would be the obvious mechanism of MR in a superconductor. A simplified analysis indicates that the effect may well be explained by field dependent proximity effect in the barrier. This explanation produces a reasonable estimate of the diffusion coefficient and the relaxation time in YBCO. Furthermore, our estimates indicate that in underdoped YBCO SNS structures, the superconductivity induced inside the barrier through the proximity effect has a short ($\sim 2-3$ nm) range, unlike the

long range proximity effect observed in optimally doped YBCO structures.

Acknowledgments: We thank Pavel Aronov for the "short" junction data of Fig. 2. This research was supported in part by the Israel Science Foundation (grant No. 1565/04), the Heinrich Hertz Minerva Center for HTSC, the Karl Stoll Chair in advanced materials, and by the Fund for the Promotion of Research at the Technion.

A . APPENDIX

For the sake of comparison with previous work, we also measured the MR of optimally doped YBCO films at temperatures close to T_c as shown in the inset of Fig. 5. In this case, the resistance showed a region linear with applied field. In the Bardeen-Stephen model [3, 10, 28], the resistance resulting from flux flow is given by $R_{\text{flux flow}} = (H/H_{c2}(T)) R_N(T)$ where H is the applied magnetic field and $R_N(T)$ is the normal state resistance at temperature T , extrapolated from the RT plot close to T_c . Using this model, we extracted the temperature dependence of H_{c2} near T_c . Our results show good agreement with previous measurements by Kunchur et al. and Ossandon et al. [29, 30], which are also plotted in Fig. 5. At temperatures much lower than T_c however, no measurable MR in the YBCO film was observed. Therefore, at low temperatures where the junctions of Fig. 3 were measured, flux flow in the YBCO electrodes does not contribute to the MR. This conclusion holds independent of the oxygen doping level of the YBCO.

-
- [1] P.G. deGennes, Rev. Mod. Phys. 36, 225 (1964).
 - [2] G. Deutscher and P.G. deGennes, in Superconductivity, edited by R.D. Parks (Dekker, New York, 1966), pp. 1005-1034.
 - [3] M. Tinkham, Introduction to Superconductivity (McGraw-Hill, 2nd edition, 1996).
 - [4] K.A. Delin and A.W. Kleinsasser, Supercond. Sci. Tech. 9, 227 (1996).
 - [5] A. Sharoni, I. Asulin, G. Koren and O. Millo, Phys. Rev. Lett. 92, 017003 (2004).
 - [6] O. Neshor and G. Koren, Appl. Phys. Lett. 74, 3392 (1999).
 - [7] O. Neshor and G. Koren, Phys. Rev. 60, 9287 (1999).
 - [8] G. Deutscher and R.W. Simon, J. Appl. Phys. 69 (7), 1 (1991).
 - [9] E. Polturak, G. Koren, D. Cohen, E. Aharoni and G. Deutscher, Phys. Rev. Lett. 67 (21), 3038 (1991).
 - [10] J. Bardeen and M.J. Stephen, Phys. Rev. 140, A1197 (1965).
 - [11] J.M. Ziman, Electrons and Phonons, ch. XII (Oxford University Press, London, 1960).
 - [12] B.I. Shklovskii and L. Efros, Sov. Phys. JETP 57 (2), 470 (1983).
 - [13] I.M. Lifshitz and V.Ya. Kirpichenkov, Sov. Phys. JETP 50 (3), 499 (1979).
 - [14] A.A. Abrikosov, Physica C 317-318, 154 (1999).
 - [15] L.I. Glazman and K.A. Matveev, Sov. Phys. JETP 67, 1276 (1988).
 - [16] L. Shkedy, P. Aronov, G. Koren and E. Polturak, Phys. Rev. B 69, 132507 (2004).
 - [17] M. Tinkham, Phys. Rev. Lett. 61 (14), 1658 (1988).
 - [18] K. Maki, in Superconductivity, edited by R.D. Parks (Dekker, New York, 1966), pp. 1035-1105.
 - [19] G. Koren, L. Shkedy and E. Polturak, Physica C 403, 45 (2004).
 - [20] Y. Ando and K. Segawa, Phys. Rev. Lett. 88 (16), 167005-1 (2002).
 - [21] I. Lubimova and G. Koren, Phys. Rev. B 68, 221519

- (2003).
- [22] N.F. Mott, *Philos. Mag.* 26, 1015 (1972); A.F. Ioffe and A.R. Regel, *Prog. Semicond.* 4, 237 (1960); J.H. Mooij, *Phys. Status Solidi A*, 17, 521 (1973).
- [23] T. Hashimoto, M. Sagoi, Y. Mizutani, J. Yoshida and K. Mizushima, *Appl. Phys. Lett.* 60, 1756 (1992).
- [24] C. Stozel, M. Siegel, G. Adrian, C. Krimmer, J. Stollner, W. Wilkens, G. Schulz and H. Adrian, *Appl. Phys. Lett.* 63, 2970 (1993).
- [25] A. Frydman and Z. Ovdychu, *Europhys. Lett.* 33, 217 (1996).
- [26] I. Bozovic, G. Logvenov, M. Verhoeven, P. Caputo, E. Goldobin, and M. R. Beasley, *Phys. Rev. Lett.* 93, 157002 (2004).
- [27] N. Gedik, J. Orenstein, Ruixing Liang, D.A. Bonn and W.N. Hardy, *Science* 300, 1410 (2003).
- [28] A.R. Stimad, C.F. Hempstead and Y.B. Kim, *Phys. Rev. Lett.* 13 (26), 794 (1964).
- [29] M.N. Kunchur, D.K. Christen and J.M. Phillips, *Phys. Rev. Lett.*, 70 (7), 998 (1993).
- [30] J.G. Ossandon, J.R. Thompson, D.K. Christen, B.C. Sales, H.R. Kerchner, J.O. Thomson, Y.R. Sun, K.W. Lay and J.E. Tkaczyk, *Phys. Rev. B* 4521, 12534 (1992).